24 GHz CMOS Transceiver with Novel T/R Switching Concept for Indoor Localization

Amin Hamidian[1], Randolf Ebelt[2], Denys Shmakov[2], Martin Vossiek[2],
Tao Zhang[1], Viswanathan Subramanian[1], Georg Boeck[1,3]

[1]Microwave Engineering Laboratory, Berlin Institute of Technology, Germany
[2]Institute of Microwaves and Photonics, University of Erlangen-Nuremberg, Germany
[3]Ferdinand-Braun-Institut, Leibniz-Institut fuer Hoechstfrequenztechnik (FBH), Germany

***Abstract* — This paper presents a 130 nm CMOS transceiver for 24 GHz wireless indoor localization. Due to a novel Rx/Tx switching concept RF-losses between receiver/ transmitter and antenna could be reduced and the T/R isolation was drastically improved. The measured transceiver chip achieves an output power and noise figure of >5 dBm and <6 dB, respectively with 2 mm^2 total chip size. The complete transceiver consumes 16 mW in the Rx- and 26 mW in the Tx-mode. The RF-transceiver-chip was integrated with a DSP-unit and mounted on a PCB for wireless indoor localization demonstration. The measured results show a distance measurement precision in the cm-range.**

***Index Terms* — 24 GHz transceiver, 130 nm CMOS, localization, secondary radar.**

I. Introduction

An attractive feature of future indoor sensor networks is the possibility to augment environmental data such as temperature or gas concentration with positioning information. This combination enables the autonomous construction of sensor maps and position depended monitor or control applications.

To be able to provide robust spatial localization for indoor applications, highly precise distance measurements are needed. A key figure for accurate ranging is a high signal-to-noise-ratio (SNR), which is a function of the power amplifier (PA) output power in the transmitter (Tx) path and the noise figure (NF) of the low noise amplifier (LNA) in the receiver (Rx) path.

The focus of this report lies in the design of the 24 GHz CMOS transceiver for a round-trip time-of-flight (RTOF) positioning system. The transceiver uses a new T/R switching concept to avoid losses between antenna and Tx output/Rx input to the greatest possible extend.

II. System Concept

The system concept utilized in this work is introduced in [1]. The network node consists of three parts: a 24 GHz RF front-end with VCO+PLL for ramp generation, a 2.4 GHz radio and a DSP board. The overall localization process can be summarized as follows:

1) Distributed clock pre-synchronization of participating nodes based on [3] and IEEE 802.15.4 standard
2) Fine synchronization as described in [2]
3) Distance measurement based on FMCW radar principle
4) Localization using distributed localization algorithm [4]

The fine-synchronization and ranging procedure relies on the evaluation of a mixing signal of frequency-modulated ramps and successive compensation of time and frequency offsets. An IEEE 802.15.4 based network synchronization procedure was implemented to ensure that the remotely transmitted and the local frequency ramps sufficiently overlap in time. The separate 2.4 GHz communication channel was chosen for reasons of power efficiency and long range capability.

The first two steps provide an accurate time reference with errors of <125 ns and 30 ps respectively [2, 3]. After

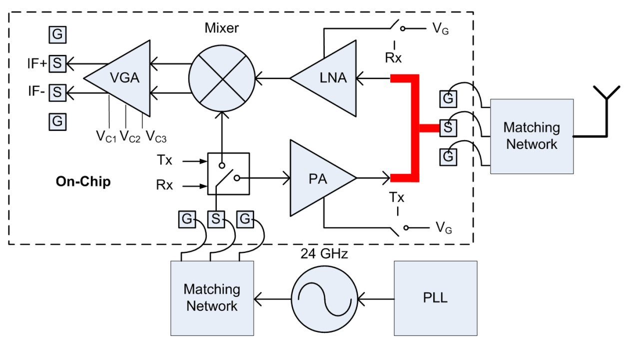

Fig. 1 Block diagram of the 24 GHz RF front-end.

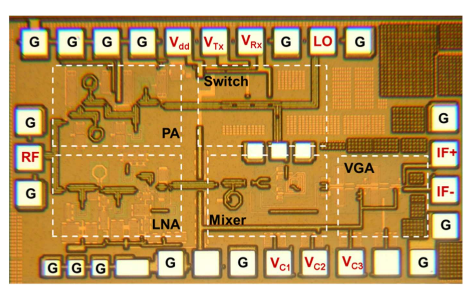

Fig. 2 Chip micrograph of the realized 24 GHz TRx.

a set of distances has been acquired, the localization algorithm in the fourth step reconstructs the coordinates of the sensor nodes.

The link budget has been calculated for <50 m distance and >15 dB SNR at the receiver. By assuming <10 dB NF for the Rx and 14 dBi antenna gain for both Tx and Rx, 0 dBm output power can be calculated for Tx.

The block diagram of the single antenna 24 GHz RF front-end is presented in Fig. 1. In this concept no switch is used for connecting the antenna to Rx and Tx. Instead, the switch is located at the LO path to switch the LO-signal between the Rx and Tx. At this point, RF-losses and limited isolation of the switch are uncritical. Additionally the LNA-biasing is switched off in the Tx-mode and the PA-biasing is switched off in the Rx-mode. Thus in the off case, LNA and PA operate as additional (nearly reactive) loads. Moreover high R/T-isolation and low power consumption is supported by this concept.

Finally, on-chip and on-board compensating techniques have been utilized to minimize the degradation of the TRx performance by packaging effects (bond wires, etc.).

II. CHIP DESIGN

The TRx RF front-end components have been realized in 130 nm CMOS technology with the total chip size of 2 mm^2 (Fig. 2). This technology provides eight metal layers and three top thick metal layers, appropriate for on-chip realization of transmission lines and inductors.

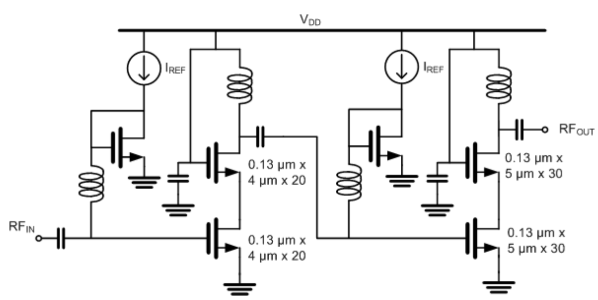

Fig. 3 Schematic of the PA.

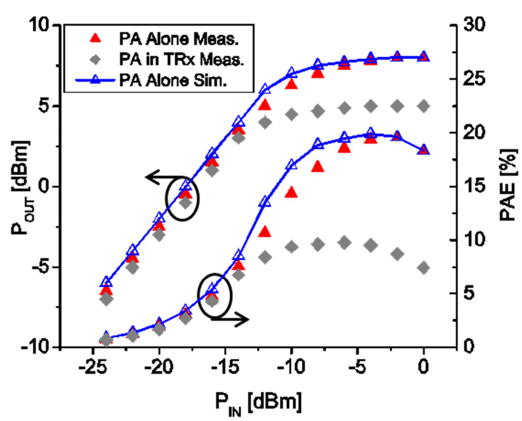

Fig. 4 Large signal measurements of the PA and Tx.

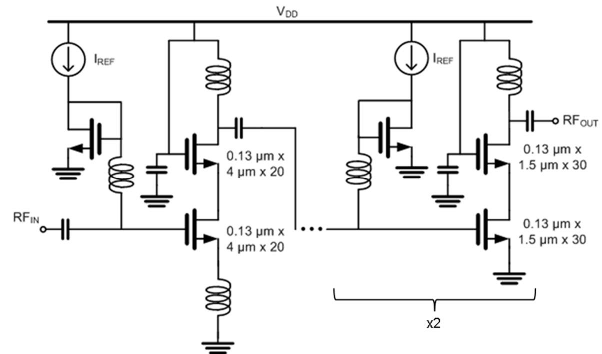

Fig. 5 Schematic of the LNA.

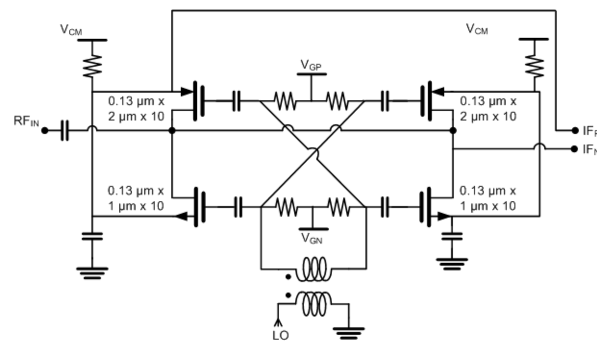

Fig. 6 Schematic of the passive mixer.

A. Transmitter

Based on linked budget calculations, around 0 dBm output power is required from the PA on system level. In order to have sufficient margin from the calculated link budget value, the PA has been designed for >7 dBm output power on chip level.

Fig. 3 presents the schematic of the designed PA. Due to high gain and stability requirements, a two stages Cascode topology was selected. The additional reactive load of the passive LNA was included during the design process. Transistor sizes and PAE were optimized by applying load-pull simulations at saturated output power. The PA has been designed, fabricated and characterized separately. The on-wafer measurements show >7 dBm output power, 18 dB gain and a peak-PAE of 20 % with 26 mW power consumption at saturation level.

Due to the on-chip bond wire compensation network the output large signal matching of the PA has been shifted in the final TRx. The TRx characterization shows >5 dBm saturated output power at Tx-mode (Fig. 4).

B. Receiver

A low IF Rx, consisting of a three stage LNA, a passive mixer and a variable gain amplifier (VGA) has been designed, fabricated and measured. The first stage of the

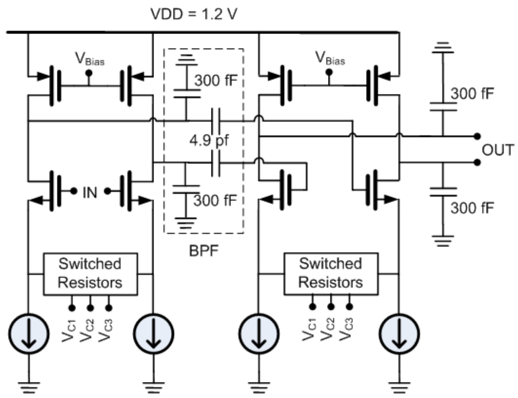

Fig. 7 Schematic of the VGA.

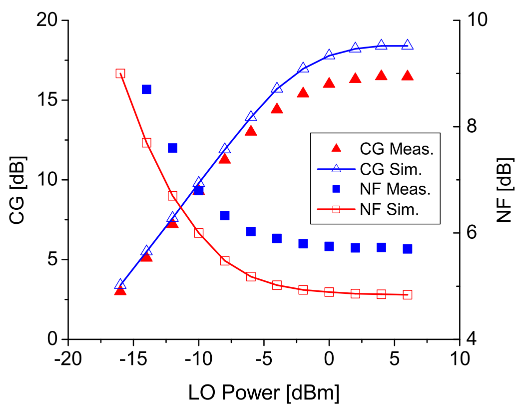

Fig. 8 Rx performance.

LNA is optimized for minimum NF while the second and third stages are designed for high gain (Fig. 5). The on-wafer measurement of the LNA alone shows 21 dB gain and 5 dB NF with 13 mW power consumption [5].

For the passive mixer a single balanced complimentary switch topology [6] has been selected (Fig. 6). This concept supports low conversion loss and consumes tolerable LO power.

Finally, Fig. 7 shows the two stages balanced VGA. It consumes 3 mW DC power and shows around 20 dB maximum gain and 35 dB dynamic range with 1 kΩ of output impedance. The VGA-gain is controlled by using three bits (V_{C1} to V_{C3}) with gain steps of 5 dB. A band pass filter (BPF) covering 1 MHz to 10 MHz is placed between the VGA stages to decouple the DC and filter out the undesirable signals.

The LO-power dependent Rx-performance is shown in Fig. 8 at medium gain of the VGA. Due to the effects of the on-chip bond wire compensation network and Rx/Tx-antenna interconnection losses (Fig. 1), the NF of the Rx is slightly worse than the NF reported in [5].

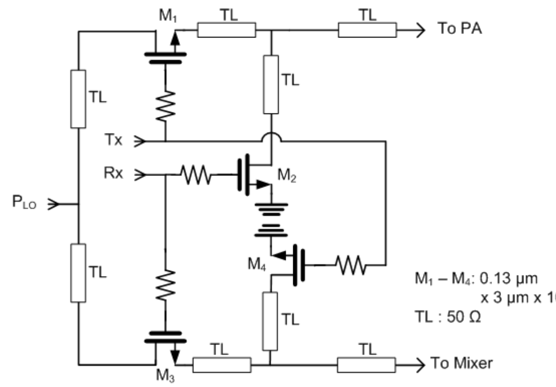

Fig. 9 Schematic of the switching circuit.

C. Switching

In order to switch between the Rx and Tx a high performance switch with floating bulk has been realized at 24 GHz (Fig. 9). The designed switch achieves <2.6 dB insertion loss and >20 dB isolation. The Rx/Tx isolation of the complete transceiver is much higher (>60 dB) because of the additional DC-switching.

IV. Demonstrator and Results

To verify the functionality of the network node, a demonstration board has been fabricated. The 24 GHz TRx board was realized on a 0.2 mm thick Rogers 4003 substrate with dielectric constant of 3.55. Also, the combined 2.4 GHz radio and DSP-board was fabricated on a 1.5 mm thick FR-4 substrate (Fig. 10).

Bond wire technique has been utilized to realize the chip-board connections (Fig. 10). As mentioned earlier, in order to compensate the inductances of the long bond wires (around 500 pH), separate matching networks have been developed on-chip and on-board. The on-chip matching network has been realized with lumped elements while the on-board compensation network utilizes transmission lines and stubs.

The main system parameters of a network node are

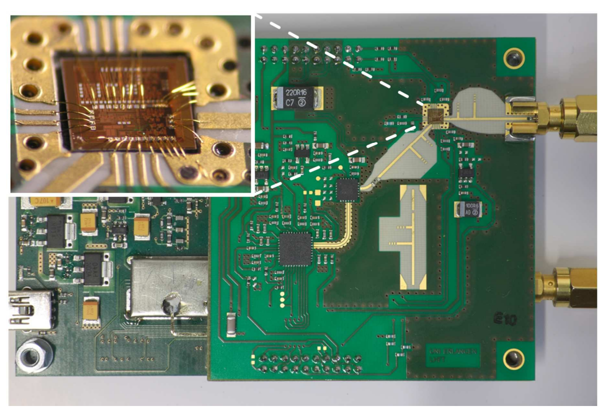

Fig. 10 Complete system with bonded 24 GHz TRx chip.

TABLE 1. NETWORK NODE PARAMETERS.

Parameter	Value	Unit
Center Frequency	24.125	GHz
Sweep Bandwidth	250	MHz
Sweep Duration	1	ms
Phase Noise @ 100 KHz	-84	dBc/Hz
Antenna Gain (Tx and Rx)	14	dBi
Measurement Rate	100	Hz

summarized in Table 1. A measurement setup consisting of two network nodes with 14 dB gain patch antennas was built up to analyze the distance measurement error.

To estimate the ranging precision, 10000 samples were taken at a fixed 2 m distance. A standard deviation of approx. 11.8 mm was determined (Fig. 12). This result almost reaches the theoretical performance limit of around 7 mm [1].

In contrast to the precision measurement, a practically more prevalent setup is a moderate multipath channel. For this purpose, the sensor node was positioned by means of a linear rail guide in steps of 20 mm along a distance of 5.5 m (Fig. 11). As expected, the multipath distortions caused the absolute ranging error to be higher than the fixed setup, but the error seldom exceeds 20 mm.

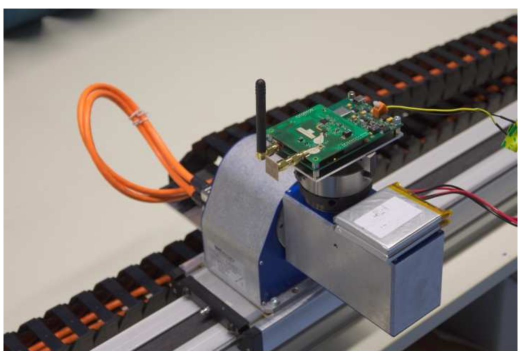

Fig. 11 System demonstrator mounted on linear guide rail.

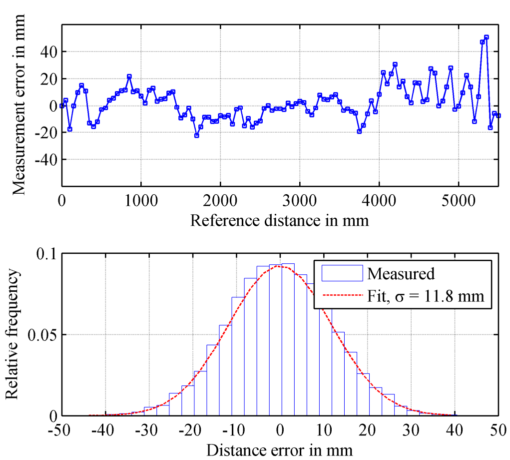

Fig. 12 Distance measurement error (top). Histogram of range measurements at 2 m distance (bottom).

A third setup with the two nodes placed at each end of a hallway is used to test the maximum usable distance. From previous experiments it is known that the minimal SNR should not drop below 15 dB to successfully fine-synchronize the two nodes. Therefore, the achieved stable measurements at maximum tested distance of 50 m showed that the SNR using only 1 ms integration time is still high enough to get robust range estimates.

VII. CONCLUSION

Through this work, the first truly wireless 24 GHz RTOF local positioning frontend with integrated CMOS transceiver has been presented. A novel on-chip T/R switch with low insertion loss and high isolation was developed. The TRx alone consumes less than 16 mW in the Rx mode and 26 mW in the Tx mode. Through three different measurement setups the system functionality has been verified. The sensor node provided excellent ranging precision near the theoretical limit, especially considering the low power consumption of the whole system.

ACKNOWLEDGEMENT

This research project is supported by a grant from the German Federal Ministry of Education and Research (BMBF) as part of the project „Low Power Wireless Sensor Network with Localization – LOWILO“, registration no. 16SV3654. The authors would like to thank Ali Sinai, Sanaz Mortazavi and Glomic GmbH for their continuous support during the project.

REFERENCES

[1] D. Shmakov et al., “Wireless Sensor Network with 24 GHz Local Positioning Transceiver,” *IEEE IMS*, pp. 17-22, June 2012.

[2] S. Röhr et al., “Precise Distance and Velocity Measurement for Real Time Locating Using a Frequency Modulated Continuous Wave Secondary Radar Approach,” *IEEE Transactions on Microwave Theory and Techniques*, vol. 56, no. 10 pp. 2329-2339, Oct. 2008.

[3] F. Kirsch et al., “Distributed Kalman filter for precise and robust clock synchronization in wireless network,” *IEEE Radio and Wireless Symposium*, pp. 482-485, 2009.

[4] R. Ebelt et al., “Wireless network-to-network localization for measuring the spatial position and orientation of vehicles”, *IEEE ICWITS 2010*, pp. 1-4, 2010.

[5] V. Subramanian et al., “Low noise 24 GHz CMOS receiver for FMCW based wireless local positioning,” *IEEE Microwave and Wireless Components Letters*, vol. 21, no. 10, pp. 553-555, Oct. 2011.

[6] S. Zhou et al., “A CMOS passive mixer with low flicker noise for low-power direct-conversion receiver,” *IEEE J. Solid-State Circ.*, vol. 40, no. 5, pp. 1084–1093, May 2005.